The endothelial cytoskeleton as a target of electroporation-based therapies

Chryso Kanthou,[1] Simona Kranjc,[2] Gregor Sersa,[2] Gill Tozer,[1] Anze Zupanic,[3] and Maja Cemazar[2]

[1]Cancer Research UK Tumour Microcirculation Group, Academic Unit of Surgical Oncology, Royal Hallamshire Hospital, University of Sheffield, Sheffield, United Kingdom; [2]Department of Experimental Oncology, Institute of Oncology Ljubljana; and [3]Faculty of Electrical Engineering, Laboratory of Biocybernetics, University of Ljubljana, Ljubljana, Slovenia

Abstract

Electroporation-based therapies, such as electrochemotherapy and electrogene therapy, result in the disruption of blood vessel networks *in vivo* and cause changes in blood flow and vascular permeability. The effects of electroporation on the cytoskeleton of cultured primary endothelial cells and on endothelial monolayer permeability were investigated to elucidate possible mechanisms involved. Human umbilical vein endothelial cells (HUVECs) were electroporated *in situ* and then immunofluorescence staining for filamentous actin, β-tubulin, vimentin, and VE-cadherin as well as Western blotting analysis of levels of phosphorylated myosin light chain and cytoskeletal proteins were performed. Endothelial permeability was determined by monitoring the passage of FITC-coupled dextran through endothelial monolayers. Exposure of endothelial cells to electric pulses resulted in a profound disruption of microfilament and microtubule cytoskeletal networks, loss of contractility, and loss of vascular endothelial cadherin from cell-to-cell junctions immediately after electroporation. These effects were voltage dependent and reversible because cytoskeletal structures recovered within 60 min of electroporation with up to 40 V, without any significant loss of cell viability. The cytoskeletal effects of electroporation were paralleled by a rapid increase in endothelial monolayer permeability. These results suggest that the remodeling of the endothelial cytoskeleton and changes in endothelial barrier function could contribute to the vascular disrupting actions of electroporation-based therapies and provide an insight into putative mechanisms responsible for the observed increase in permeability and cessation of blood flow *in vivo*. [Mol Cancer Ther 2006;5(12):3145–52]

Introduction

Electroporation involves the application of high-voltage direct-current electric pulses to cells or tissues that cause the permeabilization of the plasma membrane and, therefore, provides an effective means of increasing the uptake of molecules, such as DNA, antibodies, and drugs, into cells (1). Electroporation has been exploited for enhanced delivery of chemotherapeutic drugs, such as cisplatin and bleomycin, into tumor cells, and this process is termed electrochemotherapy (2–4). In the case of delivering DNA, the therapy is termed electrogene therapy, which is currently under preclinical and clinical investigation (5–8). Progress has also been made in DNA vaccination using electroporation, especially in the treatment of large domestic animals (9). Electrochemotherapy has high antitumor effectiveness in experimental tumors and now provides a successful means of treatment of accessible human tumors (10). Its effectiveness is thought to be primarily due to increased uptake and accumulation of chemotherapeutic drugs into the tumor cells (11, 12). Additionally, endothelial cells are potential targets of such interventions because the application of electric pulses or electrochemotherapy results in endothelial damage *in vitro* and a significant reduction in tumor blood flow *in vivo* (13–16). Such targeting of the tumor vasculature can consequently lead to a secondary cascade of tumor cell death by starving the tumor of oxygen and nutrients (17).

The cell cytoskeleton provides a basic infrastructure for maintaining cell shape and function. There are three major types of cytoskeletal structures: microtubules, actin filaments, and intermediate filaments. The endothelial cell cytoskeleton is a key target for tubulin-binding tumor vascular disrupting agents, such as the lead compound combretastatin A-4-phosphate (CA-4-P), which disrupts microtubules and causes an increase in tumor vascular permeability and a selective reduction in tumor blood flow (18–21). Changes in vascular permeability are controlled by changes in cell contractility and by the integrity of cell-to-cell junctions (22, 23). Cell contractility is regulated by actin-myosin interactions that require actin polymerization as well as phosphorylation of myosin light chain (24–26). Small GTP-binding Rho proteins are major players in regulating both contractility through myosin light chain phosphorylation and permeability in endothelial cells (22, 25, 27). Adherens junctions constitute a major type of

doi:10.1158/1535-7163.MCT-06-0410

endothelial junction responsible for the control of vascular permeability (23). These junctions are formed from the transmembrane adhesive protein vascular endothelial cadherin (VE-cadherin), which localizes as a multimeric complex at the cell border. VE-cadherin junctions are linked through a series of intracellular anchor proteins to the actinomyosin contractile system, which contributes to their disruption.

The cytoskeleton is also thought to be involved in the response of cells to electroporation (28, 29). However, the mechanisms are not known, and its role in the observed blood flow reduction in response to electroporation and electrochemotherapy, as well as electrogene therapy, have not been evaluated. Here, we investigate the reversible effects of electroporation on the cytoskeleton of cultured primary endothelial cells. We provide evidence for a profound disruption of actin and tubulin cytoskeletal networks, a loss of VE-cadherin from cell-to-cell junctions immediately after electroporation, and rapid recovery within 60 min. The cytoskeletal effects of electroporation were paralleled by a rapid increase in endothelial monolayer permeability. These results provide an insight into putative mechanisms responsible for the observed blood flow cessation *in vivo* after the application of electric pulses and suggest that the remodeling of the endothelial cytoskeleton could contribute to the observed vascular disrupting actions of electroporation-based therapies.

Materials and Methods

Materials

Monoclonal antibodies against β-tubulin (clone TUB.2.1), vimentin (clone V9), and HSP 70 (clone BRM-22), were purchased from Sigma (Poole, United Kingdom). Monoclonal anti-VE-cadherin (clone 55-7H1) was from BD Biosciences (Oxford, United Kingdom). Antiphosphospecific myosin light chain rabbit polyclonal antibody was a generous gift from Dr. James Staddon (EISAI London Research Laboratories, London, United Kingdom), and goat polyclonal antihuman myosin light chain was purchased from Santa Cruz Biotechnology (Insight Biotechnology, Wembley, United Kingdom).

Cell Culture

Human umbilical vein endothelial cells from pooled donors were obtained commercially from TCS CellWorks (Botolph Clayton, United Kingdom). Human umbilical vein endothelial cells were grown on gelatin-coated culture dishes in M199 medium supplemented with 20% FCS, 4 mmol/L L-glutamine, 80 μg/mL heparin (Sigma), and 20 μg/mL endothelial cell growth supplement (First Link, Birmingham, United Kingdom). For *in situ* electroporation experiments, cells were seeded on 2.4-cm-diameter, 0.4-μm-pore-size polycarbonate membrane transwell inserts (Costar, High Wycombe, United Kingdom) coated with 10 μg/mL human fibronectin (Invitrogen, Paisley, United Kingdom). Confluent monolayers were obtained by plating cells at a density of $5 \times 10^4/cm^2$; the medium was replaced every 48 h, and cultures were used 4 days later. To obtain subconfluent cultures, cells were plated at $5 \times 10^3/cm^2$ and were used 48 h after plating. Cells were used between the first and fourth passages.

In situ Electroporation

In situ electroporation of adherent cells was done using the *in situ* electroporation cuvette–based system (EquiBio, Middlesex, United Kingdom) attached to a custom-made electroporator. This system allows for adherent cells grown on filter inserts to be electroporated without prior detachment from their growth surface. We adopted this system to study rapid events relating to cell morphology and the cytoskeleton in endothelial cells. The system consists of a disposable cuvette designed to accept cells growing on microporous filter inserts as described above. Inserts were placed in serum-free M199 medium and were exposed to short, high-voltage square-wave electric pulses (three electric pulses of 10–80 V; frequency, 1 Hz; duration, 100 μs; and electrode gap, 4 mm). The choice of electroporation medium was based on preliminary testing of cells in several buffers and media that included Ringer bicarbonate buffer, HEPES pulsing buffer, and culture medium M199. Cytoskeletal and junctional structures of nonelectroporated cells were found to be best preserved in serum-free medium M199; thus, this was chosen as the electroporation medium. Following electroporation, cells were either processed immediately or placed in fresh M199 medium containing 20% FCS and incubated for further periods. Effective electropermeabilization was confirmed by monitoring cellular uptake of propidium iodide by fluorescence microscopy or fluorescence-activated cell sorting analysis. Voltages of ≥10 V and three pulses were found to result in optimal electropermeabilization of endothelial cells (data not shown). Cell viability, using trypan blue exclusion assay, was determined at 5 min and 24 h after electroporation of confluent endothelial cells.

Immunofluorescence Staining of the Cytoskeleton

To visualize cytoskeletal proteins, cells on filter inserts were fixed in 3.7% formaldehyde in PBS and permeabilized with 0.1% Triton X-100, and nonspecific binding sites were blocked with a mixture of 2% bovine serum albumin and 5% normal horse serum. Filters were sequentially incubated with primary monoclonal antibodies, biotinylated antimouse antibody, and FITC-labeled avidin D (Vector Laboratories, Peterborough, United Kingdom), the latter added together with 5 units/mL Texas red–conjugated phalloidin (Molecular Probes, Invitrogen, Paisley, United Kingdom) to stain for filamentous actin. Membranes were then cut away from the insert supports and mounted on glass slides in Vectashield (Vector Laboratories). Fluorescence images were taken with a Nikon Eclipse TE200 inverted microscope (Nikon, Kingston upon Thames, United Kingdom) and a cooled charge-coupled device camera (Cohu, San Diego, CA) and processed using Adobe Photoshop software.

Western Blotting and Analysis of Cytoskeletal Proteins

Cells were electroporated *in situ* as described above, and proteins were extracted at various times postelectroporation. Monolayers were washed in PBS, and cells were

lysed in the sample buffer without bromophenol blue. Proteins were quantified using Pierce bicinchoninic acid microassay kit (Perbio Science, Tattenhall, United Kingdom). Equal amounts of protein were separated on Novex Trisglycine gels (Invitrogen) and transferred to nitrocellulose membranes, and immunoreactive bands were visualized by enhanced chemiluminescence (GE Healthcare, Amersham, United Kingdom).

Endothelial Monolayer Permeability Assay

Endothelial cells were seeded on 2.4-cm-diameter, 3-μm-pore-size polycarbonate membrane transwell inserts, precoated with fibronectin as above, and allowed to reach confluency. Two days postconfluence, monolayers exhibited tight barrier properties and were subjected to electroporation. Immediately after, inserts were placed in corresponding six-well companion plates containing 2,800 μL of full medium and were replaced in the incubator. The medium (800 μL) in the upper compartment was replaced with medium containing 0.8 mg/mL FITC-coupled dextran, 40 kDa mean molecular weight (Sigma). Samples of 100 μL medium were collected from the lower compartment 30 min after electroporation, and fluorescence was monitored in an LS30 Fluorimeter (Perkin-Elmer, Wellesley, MA). Results were expressed as a percentage of fluorescence passing through control, nonelectroporated monolayers.

Statistical Analysis

Data are presented as arithmetic means ± SE. The significance of the effect was determined using post hoc Tukey's *t* test after one-way ANOVA was done; levels of <0.05 were taken as indicative of significant differences. Statistical analysis was carried out using SigmaStat statistical software (SPSS, Chicago, IL).

Results

Electroporation Causes Transient Disruption of Microtubules and Microfilaments but not Intermediate Filaments

The electroporation of adherent cells in culture normally involves prior detachment of the cells from their substratum. However, the process of detachment affects cell morphology and the cytoskeleton, and so we used endothelial cells grown on microporous filter inserts, which were then electroporated *in situ*. Cells grown on filter supports develop similar cytoskeletal structures to cells grown on conventional solid surfaces and are accessible to immunofluorescence applications.

Before electroporation, endothelial cells displayed intact actin filament and microtubule networks (Fig. 1A and B). In these cells, actin filaments predominated at the cell periphery with few fine fibers traversing the cell body (Fig. 1A). Microtubules originated from an area around the nucleus and radiated outward to the cell periphery as fine lacelike threads (Fig. 1B). Cells responded to electroporation by dissolution of actin fibers and microtubules, and these effects were evident immediately (within 5 min) after electroporation (Fig. 1C–J). Actin fibers progressively

dissociated in response to increasing voltage applications, and staining with phalloidin seemed diffuse. At the cell periphery, diffuse actin staining assumed a honeycomb-like appearance, with fine processes extending from the cell body. Microtubules progressively became fragmented and disappeared altogether at higher voltages. The disruption of these cytoskeletal components was dependent on the voltage used because 20 to 60 V led to progressively greater levels of cytoskeletal damage (Fig. 1C–J). Microtubule and microfilament networks recovered their structural composition within 1 to 2 h of electroporation at moderate voltage intensity (Fig. 1K–N). The extent of the recovery was also dependent on voltage. When electroporated with 80 V, only a fraction of cells retained the capacity to recover their cytoskeleton by 24 h (data not shown), and, in these conditions, viability was drastically reduced (see results of the subsequent section). Mitotic spindles seemed to be more resistant to disruption than normal interphase cell microtubules because spindles were found to be present when cells were exposed to voltages that caused complete interphase microtubule disruption (Fig. 1P). Similar to microtubules, vimentin intermediate filaments are organized as an extended system and stretch from the perinuclear area to the cell periphery and plasma membrane (Fig. 2B). However, unlike microtubules and microfilaments, vimentin intermediate filaments remained relatively resistant to electroporation, although some damage at peripheral areas was evident (Fig. 2D). Peripheral areas regained their original appearance within 2 h postelectroporation, which paralleled the recovery of the actin and microtubule cytoskeletons.

Loss and Recovery of Actin Filaments Correlate with Levels of Phosphorylated Myosin Light Chain, but Total Proteins Remain Unaffected

Actin stress fiber formation and contractility in nonmuscle cells, including endothelial cells, are regulated by the phosphorylation of myosin light chain, which, in turn, promotes interactions between actin and myosin, thus facilitating the formation of contractile actin-myosin filaments (24). Myosin light chain phosphorylation status was investigated in cell lysates extracted from confluent endothelial cultures subjected to 40 V. In control nonelectroporated cells, low basal levels of myosin light chain phosphorylation were detected (Fig. 3A) in accordance with their quiescent noncontractile cell morphology. Immediately after electroporation, a reduction in myosin light chain phosphorylation was detectable, which was followed by a burst in myosin light chain phosphorylation, most evident at 30 and 60 min. This burst in phosphorylation activity correlated with active cytoskeletal remodeling and the reestablishment of contractile actin filamentous structures. The total levels of myosin light chain remained unaffected, which suggests that this reduction in phosphorylated myosin light chain did not reflect changes in total protein. Total levels of actin, β-tubulin, and vimentin proteins were not down-regulated by electroporation for up to 16 h after treatment (Fig. 3B). Taken together, these data suggest that electroporation interferes with the
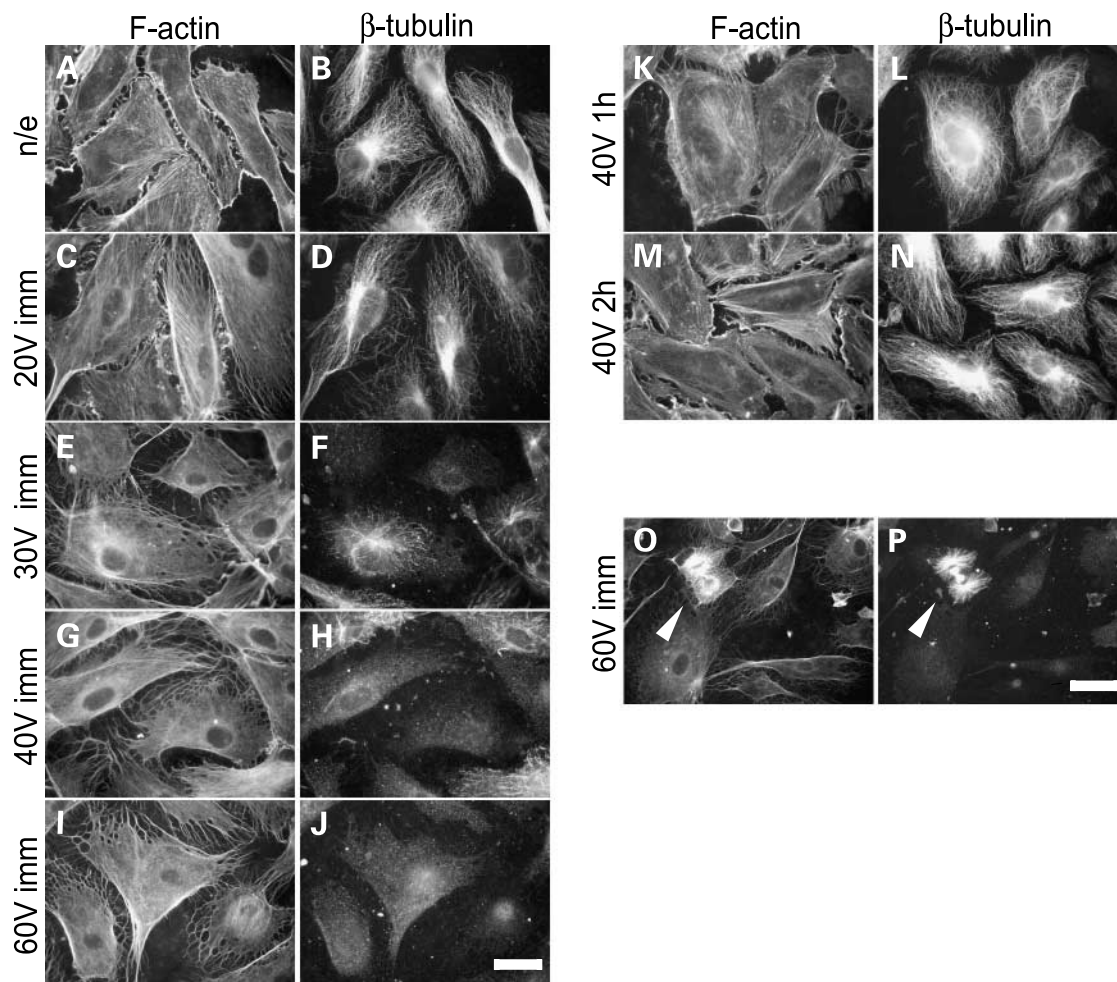
Figure 1. Electroporation causes immediate but reversible dissolution of microtubules and actin filaments. Endothelial cultures were exposed to short, high-voltage square-wave electric pulses (three electric pulses, 20–80 V, electrode gap 4 mm, 1 Hz, 100 μs). Staining of filamentous actin (*F-actin*) and microtubules of either intact nonelectroporated (*n/e*) cells (**A** and **B**), cells immediately (*imm*) after exposure to electroporation (**C** – **J, O**, and **P**), or cells that were electroporated and then allowed to recover for either 1 h (**K** and **L**) or 2 h (**M** and **N**) was done as described in Materials and Methods. **O** and **P**, *arrows*, a mitotic cell with resistant actin and spindle structures. Bar, 40 μm.

organization of actin or tubulin monomers into three-dimensional filamentous structures, but does not result in any immediate or subsequent degradation of the corresponding monomeric proteins. This observation is supported by the fact that both actin filaments and microtubules can reassemble within 1 h after electroporation (section above), which is not sufficient time for significant resynthesis of any degraded proteins. These results are further supported by the measurement of HSP 70 proteins. No increase in accumulation of this protein was observed within 16 h after electroporation, suggesting that protein damage, and possibly also DNA damage, did not occur in cells exposed to 40-V electric pulses (Fig. 3B).

The Viability of Endothelial Cells Is Not Significantly Affected by Electroporation

Endothelial cell viability was evaluated by trypan blue exclusion assay in cells detached after a 5-min recovery period after electroporation, which allows for membrane

pores to reseal (28), and at 24 h postelectroporation (Fig. 4). Voltages of up to 40 V that led to almost complete recovery of cytoskeletal structures did not cause any significant changes in cell viability either immediately or following a 24-h recovery period postelectroporation (Fig. 4). A significant drop in viability was observed when the voltage was raised to 60 V or greater. This suggests that electric voltages up to 40 V, which are sufficient to fully permeabilize the membrane and affect the cytoskeleton, do not compromise cell viability.
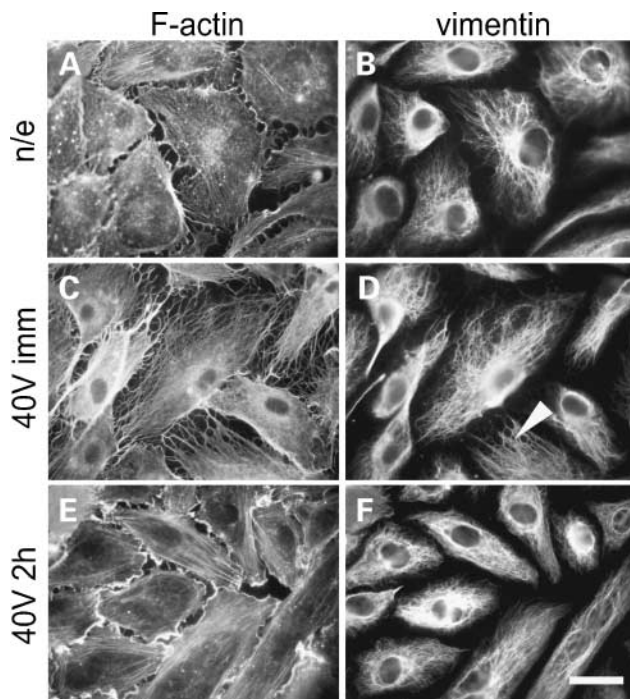
Electroporation Disrupts VE-Cadherin Endothelial Junctions and Induces a Rapid Increase in Endothelial Permeability

Adherens junctions are a specialized type of cell-to-cell junction found in endothelial cells and contribute toward the maintenance of the barrier function. To evaluate the effect of electroporation on junction stability, we used confluent cultures, as VE-cadherin localization to junctional
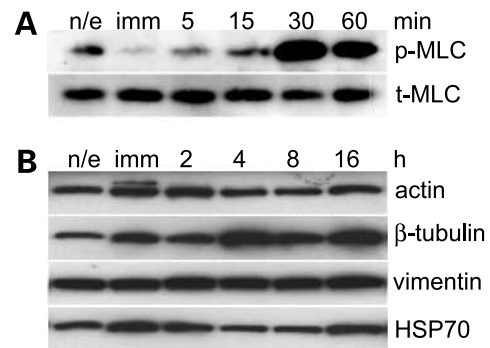
structures occurs once the cells make contact with each other (23). Figure 5B shows that VE-cadherin normally localizes at the points of cell-to-cell contact in confluent nonelectroporated cells. Loss of VE-cadherin was evident from the junctions between adjacent endothelial cells immediately after electroporation (Fig. 5D and F). Loss of junctional VE-cadherin is associated with a compromised barrier function. Monolayer permeability to FITC-coupled dextran was assessed 30 min after electroporation, and a significant, voltage- and dose-related increase in permeability was observed (Fig. 5G). This suggests that electroporation disrupts the barrier function of the endothelium by interacting with the cytoskeletal organization and junctional integrity.

Discussion

In this study, we show that electroporation of adherent human endothelial cells results in an immediate but transient disruption of interphase microtubules and actin filaments, loss of contractility, and loss of VE-cadherin from cell-to-cell junctions. These cytoskeletal changes are known to contribute toward changes in endothelial barrier function and could, therefore, account for the increase in endothelial monolayer permeability, which was observed in response to electroporation. An increase in tumor

Figure 3. Myosin light chain phosphorylation is regulated by electroporation, whereas total levels of cytoskeletal proteins remain unaffected. Confluent endothelial cultures were electroporated with 40-V electric pulses. Proteins were extracted either immediately or at the indicated times postelectroporation and analyzed by Western blotting for phosphorylated myosin light chain (*p-MLC*) and total myosin light chain protein (*t-MLC*; **A**) and for actin, β-tubulin, vimentin, and HSP 70 (**B**).

vascular permeability was previously shown to occur in response to electroporation *in vivo* (14–16). Our results, therefore, provide an insight into the molecular mechanisms involved in the vascular-damaging component of electroporation-based therapies.

Several lines of evidence suggest that the principal mechanism for the antitumor effects of electrochemotherapy is the enhanced delivery of chemotherapeutic drugs to tumor cells (11, 12). Nevertheless, it is now well established that the application of electroporation either alone or in combination with chemotherapy (electrochemotherapy) also results in tumor vascular disruption. The evidence for these vascular disrupting actions of electroporation
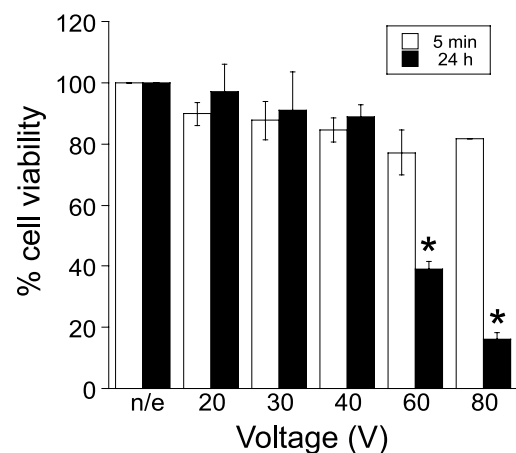

Figure 2. Vimentin intermediate microfilaments are resistant to electroporation. Endothelial cultures were electroporated with 40-V electric pulses. Staining of filamentous actin and vimentin filaments of either intact nonelectroporated cells (**A** and **B**) or cells immediately after exposure to electroporation (**C** and **D**), or at 2 h postelectroporation, was done as described in Materials and Methods. **D**, *arrow,* some peripheral damage to vimentin filaments. Bar, 40 μm.

Figure 4. The viability of endothelial cells is not significantly affected by electroporation. Endothelial cultures were electroporated with 20- to 80-V electric pulses as described for Fig. 1. Cell viability was evaluated by trypan blue exclusion assay done at either 5 min or 24 h after electroporation. Results from one of three representative experiments. Viability is expressed as a percentage of corresponding control nonelectroporated cells at 5 min or 24 h. *Columns,* mean (*n* = 4); *bars,* SE. *, values significantly different from those of corresponding nonelectroporated controls.
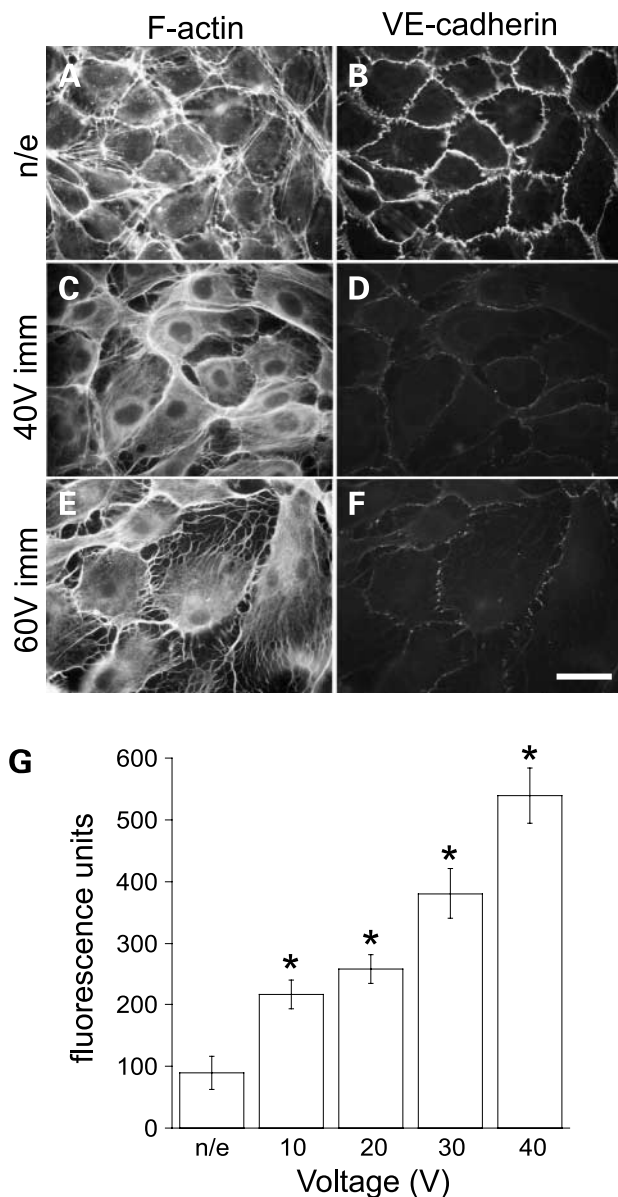
Figure 5. Electroporation disrupts VE-cadherin endothelial cell junctions and induces a rapid increase in endothelial permeability. Confluent endothelial cultures were electroporated with electric pulses of either 40 or 60 V as described in Fig. 1. Staining of filamentous actin and VE-cadherin of either intact nonelectroporated cells (**A** and **B**) or cells immediately after electroporation (**C** – **F**) was done as described in Materials and Methods. Bar, 40 μm. **G,** monolayer permeability to FITC-coupled dextran was assessed 30 min after electroporation. Results from one of three representative experiments. *Columns,* mean (*n* = 4); *bars,* SE. *, statistically significant differences compared with control non-electroporated cells.

further support for the existence of a vascular targeting element in these approaches (14–16). Furthermore, these experimental observations are supported by clinical studies demonstrating the rapid cessation of bleeding of hemorrhagic melanoma nodules immediately after electroporation (30). The application of electric pulses to normal tissues such as muscle also results in the cessation of blood flow (31). However, blood flow recovery in muscle occurs within ~30 min, whereas in tumors, flow reduction can last for up to 24 h following electroporation (16, 31, 32).

To shed some light on the underlying mechanisms of the vascular disrupting actions of electroporation-based therapies, we studied the response of the endothelial cytoskeleton to electroporation. The extent of microtubule depolymerization, the dissociation of actin filaments, as well as the disruption of adherens junctions, correlated with increasing voltage (20–60 V) of electric pulses. Interestingly, electroporation seemed to affect the same cytoskeletal targets as the vascular disrupting CA-4-P that also causes an increase in tumor vascular permeability and blood flow reduction (18, 21). Similar to CA-4-P, microtubules were rapidly disrupted by electroporation and recovered within 60 min postelectroporation. Microtubules also recover very rapidly after the removal of CA-4-P (33). These results are in accordance with the fact that microtubules are dynamic structures that undergo a continuous process of assembly and disassembly within a cell (34). Electroporation also resulted in the rapid loss of actin filaments, accompanied by an immediate reduction in myosin light chain phosphorylation and, consequently, loss of contractility. Actin remodeling is a dynamic process that is regulated by the family of small Rho-GTPases (25). These signaling molecules contribute toward not only actin filament formation but also actinomyosin contractility. In parallel to actin filament and stress fiber dissolution, basal levels of phophorylated myosin light chain were down-regulated, which implied Rho kinase inactivation. A subsequent burst in myosin light chain phosphorylation at 30 and 60 min postelectroporation correlated with the reestablishment of actin filamentous structures, confirming that the mechanism(s) responsible for the assembly of actin cytoskeletal structures remained intact. The actin cytoskeleton is also a CA-4-P target (18, 21). However, CA-4-P activates Rho-mediated signaling and leads to further myosin light chain phosphorylation and, therefore, a different actin-remodeling outcome to that of electroporation. Furthermore, whereas microtubule disruption by CA-4-P is coupled to Rho activation, their disruption by electroporation seems to uncouple Rho and inactivate Rho kinase. Activation of Rho proteins necessitates their translocation and association with membrane components (35). It is likely that electroporation inactivates Rho by preventing its association with the cell membrane. Both microtubules and actin filaments contribute toward the maintenance of the endothelial barrier function. The barrier function is controlled not only by cell-matrix tethering forces but also by the integrity of cell-to-cell junctions, including adherens junctions (22, 23). Electroporation led

comes from studies that showed a rapid increase in tumor vascular permeability and sustained reduction in tumor blood flow that was accompanied by the induction of hypoxia. In these systems, blood flow reduction and hypoxia were significantly more pronounced after electrochemotherapy with cisplatin or bleomycin, thus providing

to the disappearance of actin stress fibers, which compromises tethering of cells to their substratum and, therefore, could contribute toward the observed rapid increase in permeability. In confluent conditions, endothelial cells form cell-to-cell adhesive interactions through the cadherin family of adhesion molecules. These adhesive interactions are important for the control of not only the barrier function but also cell survival. The integrity of cadherin junctions is calcium dependent (23), and, therefore, a pulsing medium that contained free Ca^{2+} ions was selected to preserve basal cell adhesion and survival. Electroporation induced the loss of junctional VE-cadherin between neighboring cells, which was associated with increased permeability. These cytoskeletal and morphologic changes in endothelial cells were reversed within 1 h, which is in accordance with the maintenance of cell viability. Viability was, however, drastically reduced by ≥80 V because only few cells preserved the ability for complete cytoskeletal renewal within 24 h. Electroporation with up to 60 V did not affect mitotic spindles, suggesting an increased stability of spindle structures compared with interphase microtubules. This is in contrast with the reported higher sensitivity of mitotic spindles to disruption by tubulin-binding agents compared with interphase microtubules (36). Although electroporation affected microtubule and actin filament networks profoundly, there were no significant changes in intermediate vimentin filaments, indicating very little effect on the mechanical strength of the cells. Other investigators have previously shown that although electroporation disrupts the tubulin cytoskeleton of fibroblasts and Chinese hamster ovary cells, it does not alter their actin cytoskeleton (29, 37). The fact that actin filaments were found to be unaffected in fibroblasts could be due to conditions of electric pulses because Hankin and Hay (29) used exponentially decaying electric pulses. Additionally, cell type–specific properties, including the anchorage-independent nature of CHO-WTT cells, could account for these differences in response to electroporation (37). The fact that electroporation did not cause any significant changes in total levels of actin, β-tubulin, and vimentin in endothelial cells suggests that the degradation of the corresponding monomers was not triggered. Furthermore, the unchanged level of HSP 70 protein provides evidence that electroporation with up to 40 V did not elicit protein damage and, possibly, no DNA damage either. Other investigators showed that the exposure of human leukemic K562 cells to higher electric fields (from 100 to 500 V/cm) produced a weak but long-lasting expression of HSP 70-2 mRNA (38). This could imply that our electroporation conditions were not sufficient to stimulate detectable induction of stress proteins.

In the current study, permeabilization of adherent endothelial cells was achieved with 20 to 80 V, representing electric field strengths of 50 to 200 V/cm. This is in contrast to the significantly higher field intensities, ranging between 800 and 1,800 V/cm, previously used for electropermeabilization of endothelial cells in suspension (13) or indeed for tumor electropermeabilization *in vivo* (3, 10, 13). The

relatively low electric fields required for electropermeabilization in our study can be explained by the shape and organization, as well as the density of endothelial cells when in a monolayer. Susil et al. (39) have shown that neighboring cells in the same plane decrease the available extracellular current pathways; therefore, the current density and potential drop around the cells increases. Furthermore, the maximum transmembrane voltage for a monolayer of spherical cells oriented perpendicularly to the electric field increases by a factor of ~1.4. Because there is even less space for the electric current in a confluent endothelial monolayer, then the increase in the transmembrane voltage would be expected to be much higher. The current pathways in our experimental setting are additionally reduced by the filter membrane support, which contributes to the higher transmembrane voltage on the basal side of the cells (40).

In conclusion, electroporation of an adherent endothelial monolayer induced the disruption of cytoskeletal structures and increased permeability. Our observations could offer an explanation for the immediate increase in permeability and associated blood flow reduction after electroporation and electrochemotherapy *in vivo*. Owing to known differences between the normal and tumor vasculature, we can speculate that these changes would persist longer in the tumor and could, in part, provide an explanation for the observed antitumor effectiveness of electroporation-based therapies.

References

1. Mir LM. Therapeutic perspectives of *in vivo* cell electropermeabilization. Bioelectrochemistry 2000;53:1–10.

2. Belehradek J, Jr., Orlowski S, Poddevin B, Paoletti C, Mir LM. Electrochemotherapy of spontaneous mammary tumours in mice. Cancer 1991;27:73–6.

3. Sersa G, Cemazar M, Miklavcic D. Antitumor effectiveness of electrochemotherapy with *cis*-diamminedichloroplatinum(II) in mice. Cancer Res 1995;55:3450–5.

4. Mir LM, Orlowski S. Mechanisms of electrochemotherapy. Adv Drug Deliv Rev 1999;35:107–18.

5. Cemazar M, Sersa G, Wilson J, et al. Effective gene transfer to solid tumors using different nonviral gene delivery techniques: electroporation, liposomes and integrin-targeted vector. Cancer Gene Ther 2002;9:399–406.

6. Heller R, Jaroszeski M, Atkin A, et al. *In vivo* gene electroinjection and expression in rat liver. FEBS Lett 1996;389:225–8.

7. Rols MP, Delteil C, Golzio M, Dumond P, Cros S, Teissie J. *In vivo* electrically mediated protein and gene transfer in murine melanoma. Nat Biotechnol 1998;16:168–71.

8. Mir LM, Moller PH, Andre F, Gehl J. Electric pulse-mediated gene delivery to various animal tissues. Adv Genet 2005;54:83–114.

9. Babiuk LA, Pontarollo R, Babiuk S, Loehr B, van Drunen Little-van den Hurk S. Induction of immune responses by DNA vaccines in large animals. Vaccine 2003;21:649–85.

10. Byrne CM, Thompson JF. Role of electrochemotherapy in the treatment of metastatic melanoma and other metastatic and primary skin tumors. Expert Rev Anticancer Ther 2006;6:671–8.

11. Belehradek J, Jr., Orlowski S, Ramirez LH, Pron G, Poddevin B, Mir LM. Electropermeabilization of cells in tissues assessed by the qualitative

and quantitative electroloading of bleomycin. Biochim Biophys Acta 1994; 1190:155 – 63.

12. Cemazar M, Miklavcic D, Scancar J, Dolzan V, Golouh R, Sersa G. Increased platinum accumulation in SA-1 tumour cells after *in vivo* electrochemotherapy with cisplatin. Br J Cancer 1999;79:1386 – 91.

13. Cemazar M, Parkins CS, Holder AL, Chaplin DJ, Tozer GM, Sersa G. Electroporation of human microvascular endothelial cells: evidence for an anti-vascular mechanism of electrochemotherapy. Br J Cancer 2001;84: 565 – 70.

14. Sersa G, Cemazar M, Miklavcic D, Chaplin DJ. Tumor blood flow modifying effect of electrochemotherapy with bleomycin. Anticancer Res 1999;19:4017 – 22.

15. Sersa G, Cemazar M, Parkins CS, Chaplin DJ. Tumour blood flow changes induced by application of electric pulses. Eur J Cancer 1999;35: 672 – 7.

16. Sersa G, Krzic M, Sentjurc M, et al. Reduced blood flow and oxygenation in SA-1 tumours after electrochemotherapy with cisplatin. Br J Cancer 2002;87:1047 – 54.

17. Denekamp J. Vascular attack as a therapeutic strategy for cancer. Cancer Metastasis Rev 1990;9:267 – 82.

18. Kanthou C, Tozer GM. The vascular disrupting agent combretastatin A-4 phosphate induces reorganization of the actin cytoskeleton and early membrane blebbing in human endothelial cells. Blood 2002;99: 2060 – 9.

19. Tozer GM, Prise VE, Wilson J, et al. Combretastatin A-4 phosphate as a tumor vascular-targeting agent: early effects in tumors and normal tissues. Cancer Res 1999;59:1626 – 34.

20. Tozer GM, Prise VE, Wilson J, et al. Mechanisms associated with tumor vascular shut-down induced by combretastatin A-4 phosphate: intravital microscopy and measurement of vascular permeability. Cancer Res 2001;61:6413 – 22.

21. Tozer GM, Kanthou C, Baguley BC. Disrupting tumour blood vessels. Nat Rev Cancer 2005;5:423 – 35.

22. Wojciak-Stothard B, Ridley AJ. Rho GTPases and the regulation of endothelial permeability. Vasc Pharmacol 2002;39:187 – 99.

23. Bazzoni G, Dejana E. Endothelial cell-to-cell junctions: molecular organisation and role in vascular homeostasis. Physiol Rev 2004;84: 869 – 901.

24. Kohama K, Ye LH, Hayakawa K, Okagaki T. Myosin light chain kinase: an actin-binding protein that regulates an ATP-dependent interaction with myosin. Trends Pharmacol Sci 1996;17:284 – 7.

25. Ridley AJ, Hall A. The small GTP-binding protein Rho regulates the assembly of focal adhesions and actin stress fibers in response to growth factors. Cell 1992;70:389 – 99.

26. Amano M, Ito M, Kimura K, et al. Phosphorylation and activation of myosin by Rho-associated kinase (Rho-kinase). J Biol Chem 1996;271: 20246 – 9.

27. van Nieuw Amerongen GP, van Hinsbergh VW. Cytoskeletal effects of rho-like small guanine nucleotide-binding proteins in the vascular system. Arterioscler Thromb Vasc Biol 2001;21:300 – 11.

28. Teissie J, Rols MP. Manipulation of cell cytoskeleton affects the lifetime of cell membrane electropermeabilization. Ann N Y Acad Sci 1994; 720:98 – 110.

29. Harkin DG, Hay ED. Effects of electroporation on the tubulin cytoskeleton and directed migration of corneal fibroblasts cultured within collagen matrices. Cell Motil Cytoskeleton 1996;35:345 – 57.

30. Gehl J, Geertsen PF. Efficient palliation of haemorrhaging malignant melanoma skin metastases by electrochemotherapy. Melanoma Res 2000; 10:585 – 9.

31. Gehl J, Skovsgaard T, Mir LM. Vascular reactions to *in vivo* electroporation: characterization and consequences for drug and gene delivery. Biochim Biophys Acta 2002;1569:51 – 8.

32. Kranjc S, Cemazar M, Grosel A, Scancar J, Sersa G. Electroporation of LPB sarcoma cells *in vitro* and tumors *in vivo* increases the radiosensitizing effect of cisplatin. Anticancer Res 2003;23:275 – 81.

33. Galbraith SM, Chaplin DJ, Lee F, et al. Effects of combretastatin A4 phosphate on endothelial cell morphology *in vitro* and relationship to tumour vascular targeting activity *in vivo*. Anticancer Res 2001;21: 93 – 102.

34. Amos LA, Schlieper D. Microtubules and maps. Adv Protein Chem 2005;71:257 – 98.

35. Bokoch GM, Bohl BP, Chuang TH. Guanine nucleotide exchange regulates membrane translocation of Rac/Rho GTP-binding proteins. J Biol Chem 1994;269:31674 – 9.

36. Wilson L, Jordan MA. Microtubule dynamics: taking aim at a moving target. Chem Biol 1995;2:569 – 73.

37. Blangero C, Rols MP, Teissie J. Cytoskeletal reorganization during electric-field-induced fusion of Chinese hamster ovary cells grown in monolayers. Biochim Biophys Acta 1989;981:295 – 302.

38. Dressel R, Baraki H, Langer F, Gunther E. Reduced susceptibility of electroporated tumor cell lines to killing by cytotoxic lymphocytes. Biochem Biophys Res Commun 1998;250:259 – 63.

39. Susil R, Semrov D, Miklavcic D. Electric field-induced transmembrane potential depends on cell density and organization. Electro Magnetobiol 1998;17:391 – 9.

40. Sugar IP, Lindesay J, Schmukler RE. Phenomenological theory of low-voltage electroporation. Electric field calculations. J Phys Chem B 2003; 107:3862 – 70.